

VIII. MICROWAVE ELECTRONICS*

Prof. L. D. Smullin
Prof. H. A. Haus
L. C. Bahiana

A. Bers
P. Chorney
T. J. Fessenden
W. D. Getty

S. Holly
R. Litwin
A. Zacharias

A. KLYSTRONS†

1. STAGGER-TUNED KLYSTRONS

This work has been summarized in an Sc.D. thesis, entitled "Interaction of Electrons with Electromagnetic Fields of Gaps, with Application to Multicavity Klystrons," presented to the Department of Electrical Engineering, M.I.T., May 1959.

A. Bers

2. HIGH-EFFICIENCY BUNCHING (THE SQUEEZER)

A model of a squeezer has been built and experiments are being made (see Fig. VIII-1). A 10-kv pulsed shielded cathode gun of perveance 10^{-6} is used to form the beam. The output cavity is very heavily loaded so that it can be used as an "ammeter" (low-impedance) to measure beam current. A polystyrene double-slug tuner allows us to vary the gap impedance over a range of approximately 36:1.

The best efficiency obtained thus far has been approximately 30 per cent; but there was a strong multipactor discharge in the output cavity at this power level. The present effort is aimed at eliminating the multipactor discharge so that the true limiting efficiency can be determined.

L. D. Smullin, S. Holly

B. NOISE IN ELECTRON BEAMS

The measurements described (1) in Quarterly Progress Report No. 53, have been continued. Another Bell Telephone Laboratories low-noise electron gun was installed in the apparatus and the cathode activated. Measurements were made with only one beam current, 75 μ a. The profile-shaping electrode voltage (V_{BFE}) was varied from +5 to +18 volts; the first anode voltage (V_1) was varied to keep the beam current at 75 μ a. Measurements of S and Π/S were made at five conditions of V_{BFE} and V_1 .

*This research was supported in part by Purchase Order DDL-B222 with Lincoln Laboratory, a center for research operated by M.I.T., which is supported by the U.S. Air Force under Air Force Contract AF19(604)-5200.

†This work was supported in part by the U.S. Navy (Office of Naval Research under Contract Nonr-1841(49)). Reproduction in whole or in part is permitted for any purpose of the United States Government.

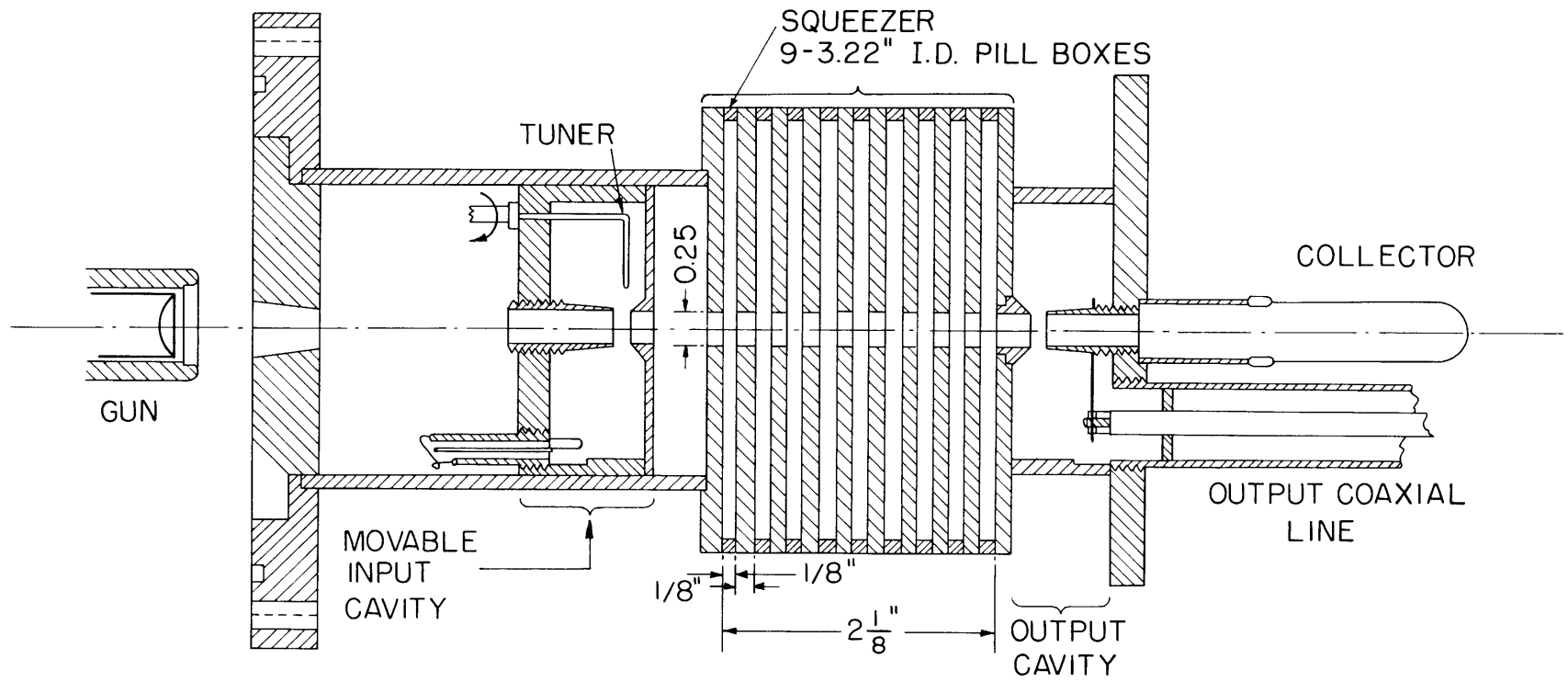


Fig. VIII-1. Block diagram of squeezer experiment.

The $V_{BFE}-V_1$ characteristic for constant beam current of $75 \mu a$ is plotted in Fig. VIII-2. The noise-parameter values that were obtained are plotted in Figs. VIII-3 and VIII-4.

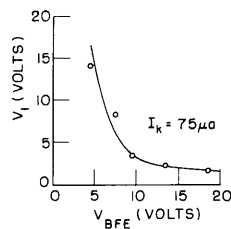


Fig. VIII-2. Anode characteristic at constant beam current.

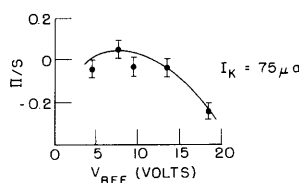


Fig. VIII-3. Variation of Π/S at constant beam current.

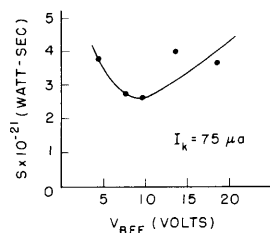


Fig. VIII-4. Variation of S at constant beam current.

Measurements have been made by Currie and Forster (2) on low-noise backward-wave amplifiers with the use of an electron gun of design similar to that of the BTL gun. They measured the minimum noise figure obtainable from the amplifier while V_{BFE} and V_1 were varied to keep the beam current fixed. Currie and Forster's results can thus be interpreted as a measure of the quantity $(S-\Pi)$ as a function of V_{BFE} .

In Fig. VIII-5 a comparison between our measured results of $S(1 - \Pi/S)$ and Currie and Forster's data (2) on $(S-\Pi)$ is made. The abscissa, V_{BFE} , is not changed from Currie and Forster's results, since the abrupt change of slope in their curve of V_1 versus V_{BFE} occurred at the same value of V_{BFE} as the break in our curve did. The value of $(S-\Pi)$ at the minimum of Currie and Forster's curve of $(S-\Pi)$ versus V_{BFE} is multiplied by a factor to make it agree with our minimum value of $S(1 - \Pi/S)$. Currie and Forster's curve is then scaled by this factor and drawn as a solid line in Fig. VIII-5. The points on the curve are our values of $S(1 - \Pi/S)$.

In a previous report (1), a discrepancy between the measured and calculated values of the shot-noise calibration was described. During the past quarter, this discrepancy was resolved. An error exists in the manner in which bandwidth was taken into account in the calculation of the calibration. This should have been discovered when a

(VIII. MICROWAVE ELECTRONICS)

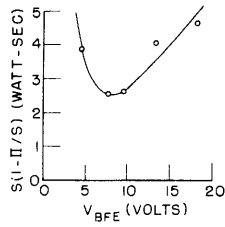


Fig. VIII-5. Comparison of measured results with data of Currie and Forster.
○, Measured points.
—, Data from Currie and Forster of (S-II) scaled to match measured value of $S(1 - \Pi/S)$ at $V_{BFE} = 7.7$.

narrow-band-filter cavity was used at the input to the radiometer as was discussed in the last report. However, the bandwidth of this cavity was found to be wider than we had thought. When the bandwidth of the entire system was measured with the excited cavity used as input, the calculated calibration agreed with the measured calibration, within 1 db, when either a temperature-limited beam or North interception was used.

The noise measurements described here were used as the basis for the author's E.E. thesis entitled, "Noise Measurements on Electron Beams at 3000 mc," Department of Electrical Engineering, M.I.T., May 1959.

A. Zacharias

References

1. A. Zacharias, Noise measurements on electron beams at 3000 mc, Quarterly Progress Report No. 53, Research Laboratory of Electronics, M.I.T., April 15, 1959, p. 51.
2. M. R. Currie and D. C. Forster, New mechanism of noise reduction in electron beams, J. Appl. Phys. 30, 94 (1959).

C. MICROWAVE CIRCUITS

1. RESONATING OBSTACLES FOR CYLINDRICAL-WAVEGUIDE DELAY LINE

Properties of several diaphragms suitable for resonating obstacles in cylindrical waveguides, which could also be used as delay-lines elements, were investigated. Most of them were of the form shown in Fig. VIII-6. Essentially, they were composed of a capacitive ring of outer and inner radii b and c , and of inductive strips of width d . (In the waveguide of radius a , the TM_{01} mode (the lowest symmetrical mode) was excited.) In order to tune the diaphragm to a particular resonant frequency, or to obtain the desired admittance of the resonant circuit, slots of width e and length l were provided. If the lengths of the slots are increased, the inductances of the strips increase. Figure VIII-7 gives an example of the tuning action of the slots. The normalized characteristic dimensions of the diaphragm in this case were: $\frac{b}{a} = 0.78$; $\frac{c}{a} = 0.26$; $\frac{d}{a} = 0.16$; $\frac{e}{a} = 0.03$.

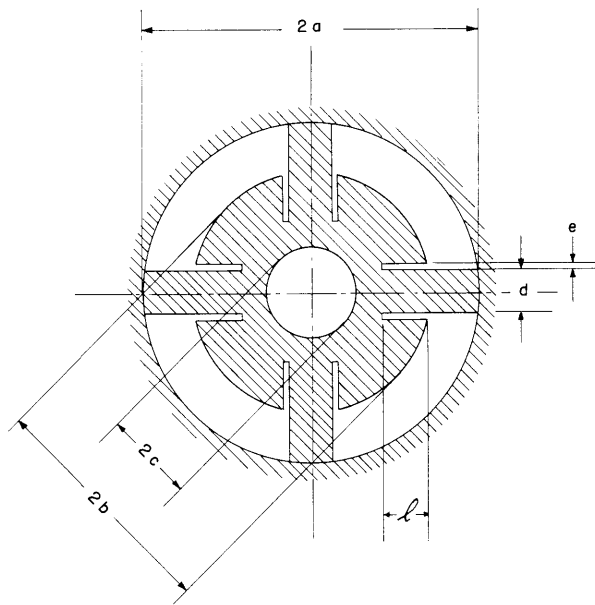


Fig. VIII-6. A resonating diaphragm.

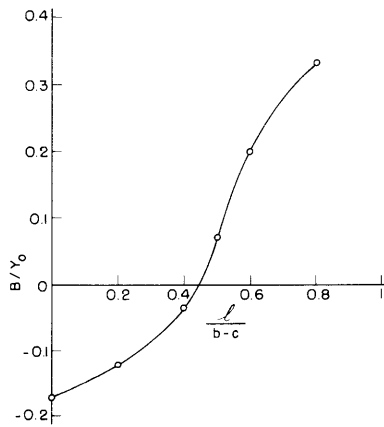


Fig. VIII-7. Normalized susceptance of a diaphragm versus normalized slot lengths.

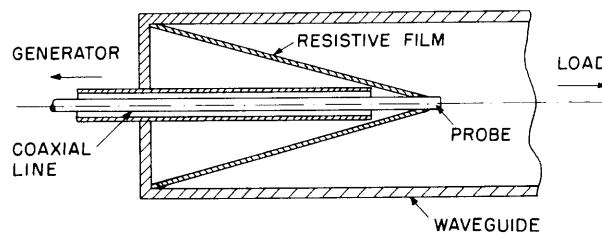


Fig. VIII-8. Coaxial-to-waveguide transition.

(VIII. MICROWAVE ELECTRONICS)

In order to excite a pure TM_{01} mode, that is, to reduce incidental coupling to the $TE_{1,1}$ circular waveguide mode, the probe shown in Fig. VIII-8 was used.

R. Litwin

2. COUPLING OF MODES IN UNIFORM COMPOSITE WAVEGUIDES

a. Introduction

The expression "uniform composite waveguide" is used in this discussion to describe any hollow metallic structure with cylindrical symmetry, filled with two or more homogeneous materials. Both the structure and the materials are uniform in the direction of propagation. Familiar examples of uniform composite waveguides are waveguides partly filled with dielectric or magnetic material. The solution of the boundary-value problem in such waveguides invariably leads to transcendental equations. Numerical solutions for a few particular cases have been published (1).

A different formulation of the problem is presented here and applied to the case of lossless waveguides containing two media. The fields are expressed in terms of the natural modes of two hypothetical waveguides, found by imposing short-circuit ($\bar{n} \times \bar{E} = 0$) or open-circuit ($\bar{n} \times \bar{H} = 0$) constraints at the boundary between the two media. Maxwell's equations are then transformed, by the use of conventional techniques, into an infinite set of coupled transmission line equations. Although this formulation is completely general, its practical usefulness stems from the possibility of obtaining approximate solutions without cumbersome numerical computation.

b. Formulation of the Problem

Figure VIII-9 shows a cross section of a composite waveguide. Surface S_1 is the metallic envelope. Surface S_2 is the boundary between the two media. The solution of Maxwell's

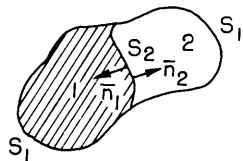


Fig. VIII-9. Composite waveguide of arbitrary cross section.

equations in medium 1 or medium 2 is unique if either $\bar{n} \times \bar{E}$ or $\bar{n} \times \bar{H}$ is specified over the boundary. Let $\bar{n} \times \bar{E}_2(S_2)$, where \bar{E}_2 is the unknown field in region 2, be specified over S_2 . Then we can solve Maxwell's equations in medium 1. In order to do this, surface S_2 is replaced by a metallic wall S (short circuit, with $\bar{n} \times \bar{E} = 0$) and a magnetic current sheet, $\bar{K}_M = \bar{n} \times \bar{E}_2(S_2)$. Mathematically, this is equi-

valent to transforming a homogeneous differential equation with inhomogeneous boundary conditions into an inhomogeneous one with homogeneous boundary conditions. Next, we solve Maxwell's equations in medium 2, with $\bar{n} \times \bar{H}_1(S_2)$ specified over S_2 . This time,

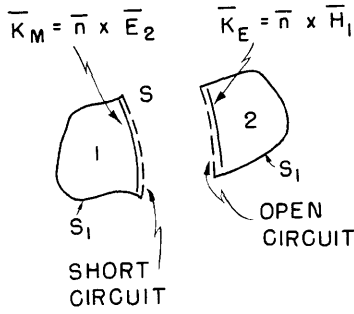


Fig. VIII-10. Equivalent driving currents and boundary constraints.

we replace the surface S_2 by a magnetic wall S (or open-circuit, with $\bar{n} \times \bar{H} = 0$) and an electric current sheet $\bar{K}_E = \bar{n} \times \bar{H}_1(S_2)$.

By this procedure, we have split the original boundary-value problem into one of two conventional waveguides driven by electric or magnetic surface currents (Fig. VIII-10). The two hypothetical waveguides will be called sub-waveguides 1 and 2. The fields in the

subwaveguides can be expanded in terms of E-modes and H-modes that satisfy either short-circuit or open-circuit boundary conditions at the common boundary. In terms of these modes, the transverse fields in either subwaveguide can be expressed (2) as

$$\bar{E}_t = \sum_{j=1}^{\infty} V_j(z) \bar{e}_{tj}(x, y)$$

$$\bar{H}_t = \sum_{j=1}^{\infty} J_j(z) \bar{h}_{tj}(x, y)$$

where

$$V_j(z) = \iint (\bar{E}_t \cdot \bar{h}_{tj} \times \bar{i}_z) da$$

$$J_j(z) = \iint (\bar{H}_t \cdot \bar{i}_z \times \bar{e}_{tj}) da$$

and the integration is extended over the cross section of the subwaveguide. The coupling equations (3) for a composite waveguide containing two media are

$$\left. \begin{aligned} -\frac{dV_j}{dz} &= M_{jj} J_j + M_{jk} J_k \\ -\frac{dJ_j}{dz} &= N_{jj} V_j + N_{jk} V_k \end{aligned} \right\} \quad (1)$$

$$\left. \begin{aligned} -\frac{dV_k}{dz} &= M_{kk} J_k + M_{kj} J_j \\ -\frac{dJ_k}{dz} &= N_{kk} V_k + N_{kj} V_j \end{aligned} \right\} \quad (2)$$

where

(VIII. MICROWAVE ELECTRONICS)

$$\begin{aligned}
 M_{jj} &\equiv j\omega\mu_j + \frac{p_{ej}^2}{j\omega\epsilon_j} + \frac{1}{j\omega\epsilon_k} \int (\bar{h}_{tj} \cdot \bar{h}_{tj}) ds & M_{jk} &\equiv \frac{\Gamma_{ek}}{j\omega\epsilon_k} \int (\bar{n} \cdot \bar{e}_{zk} \times \bar{h}_{tj}) ds \\
 N_{jj} &\equiv j\omega\epsilon_j + \frac{p_{Hj}^2}{j\omega\mu_j} & N_{jk} &\equiv \frac{\Gamma_{Hj}}{j\omega\mu_j} \int (\bar{n} \cdot \bar{e}_{tk} \times \bar{h}_{zj}) ds \\
 M_{kk} &\equiv j\omega\mu_k + \frac{p_{ek}^2}{j\omega\epsilon_k} & M_{kj} &\equiv \frac{\Gamma_{ek}}{j\omega\epsilon_k} \int (\bar{n} \cdot \bar{e}_{zk} \times \bar{h}_{tj}) ds \\
 N_{kk} &\equiv j\omega\epsilon_k + \frac{p_{Hk}^2}{j\omega\mu_k} + \frac{1}{j\omega\mu_j} \int (\bar{e}_{tk} \cdot \bar{e}_{tk}) ds & N_{kj} &\equiv \frac{\Gamma_{Hj}}{j\omega\mu_j} \int (\bar{n} \cdot \bar{e}_{tk} \times \bar{h}_{zj}) ds
 \end{aligned}$$

The integrals are taken along the boundary, in the transverse plane. The subscript j has been retained for the subwaveguide with the short circuit imposed at the wall, and the subscript k has been used for the subwaveguide with the open circuit imposed at the boundary.

To illustrate the method, we have calculated the propagation constants of the fundamental mode of a rectangular waveguide half-filled with dielectric of dielectric constant $\epsilon = 2.45$ (Fig. VIII-11). The fundamental mode can be found by coupling the TE_{10} modes of each subwaveguide. The approximation is good if we choose short-circuit modes in

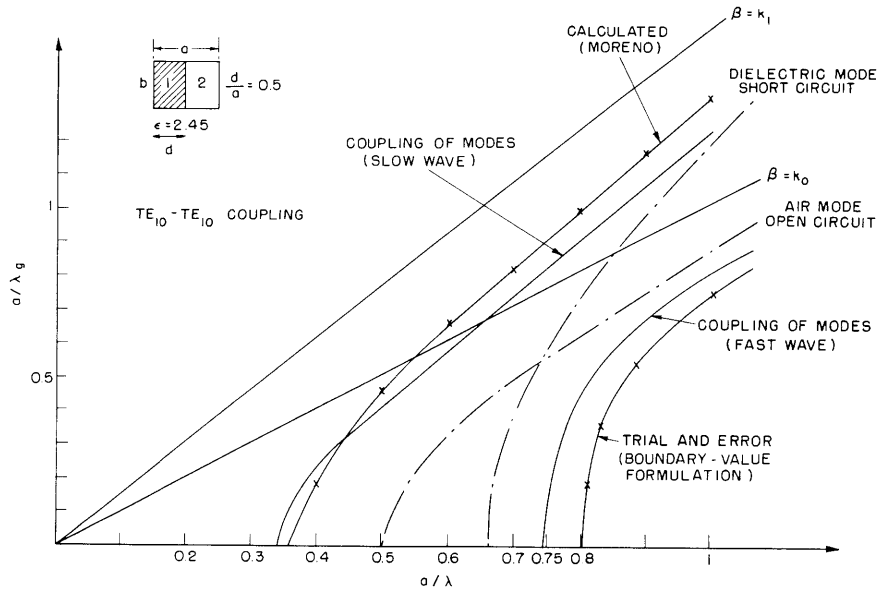


Fig. VIII-11. Propagation in rectangular waveguide half-filled with dielectric.

the dielectric (subwaveguide 1) and open-circuit modes in air (subwaveguide 2). For this simple case, the coupling equations lead to

$$\Gamma^2 = \frac{1}{2} \left[\left(\Gamma_1^2 + \Gamma_2^2 \right) \pm \left(\left(\Gamma_1^2 - \Gamma_2^2 \right) + 4K^2 \right)^{1/2} \right]$$

where

$$\Gamma_1^2 = p_1^2 - k_1^2 = \left(\frac{\pi}{d} \right)^2 - \left(\frac{\epsilon_1}{\epsilon_0} \right) k_0^2$$

$$\Gamma_2^2 = p_2^2 - k_0^2 = \left(\frac{\pi}{2d} \right)^2 - k_0^2$$

$$k_0^2 = \omega^2 \mu_0 \epsilon_0$$

$$K = \frac{\pi}{d} [d(a-d)]^{-1/2} = \frac{4\pi}{a}$$

The results of exact computation based on the boundary-value formulation are also shown in Fig. VIII-11.

L. C. Bahiana

References

1. T. Moreno, Microwave Transmission Design Data (Dover Publications, Inc., New York, 1958), p. 192.
2. H. A. Haus, Microwave Circuits, Course 6.621 Class Notes, Massachusetts Institute of Technology, 1959.
3. L. C. Bahiana, Coupling of modes in uniform composite guides, Internal Report, Microwave Laboratory, Research Laboratory of Electronics, M.I.T., 1959.